Research Article | Vol. 9, No. 7 / 1 July 2019 / Optical Materials Express 2870

Optical Materials EXPRESS

Spectral reflectivity crossover at the metamagnetic transition in FeRh thin films

S. P. BENNETT,[1] M. CURRIE,[2] O. M. J VAN 'T ERVE,[1] AND I. I. MAZIN[1]

[1] *Materials Science and Technology Division, The U.S. Naval Research Laboratory, Washington, DC 20375, USA*

[2] *Optical Sciences Division, The U.S. Naval Research Laboratory, Washington, DC 20375, USA*

[*] *Steven.Bennett@nrl.navy.mil*

Abstract: Metamagnetic transition in FeRh has been subject to many investigations. Several methods have been employed to address various characteristics as they change across this transition, such as SQUID magnetometry, neutron scattering, electrical transport, synchrotron X-rays, scanning tunneling microscopy, magneto-optic Kerr effect, etc. In this paper we investigate the frequency dependent reflectance, which is a fast and easy probe, to find clear and distinct signatures of this transition. To this end, our first principle calculations reveal that the dramatic difference in electronic structure between the ferro- and antiferromagnetic phases of FeRh leads to a characteristic crossover in the energy dependence whereby the reflectivity difference between the two phases changes sign at E=~0.79 eV (1400 nm). To verify these predictions, we have measured the optical reflectance of FeRh thin films across the metamagnetic transition, and found a close agreement with the predicted effect. These measurements not only confirm the calculated electronic structure of FeRh, but also reveal an effect that can be used for a fast and easy direct detection of the transition by probing the crossover optically in energy space, without resorting to complicated magneto optical probes which only show a signature of the surface magnetism. This also may be used as a unique probe of the dynamics of carriers by temporal studies in different regions, (from energies near the relaxation frequency to those above the plasma frequency).

1. Introduction

Thin films of Fe_xRh_{1-x} (x=~0.48-0.52) undergo a metamagnetic phase transition from antiferromagnetic (AF) to ferromagnetic (FM) ordering at a temperature of ~360 K. There has been a plethora of recent interest in the material for applications in the electric field control of magnetism [1–3], strain induced phase transitional triggering [4,5], HAMR magnetic recording [6], high speed all optical magnetization switching [7], and magnetic order control at the nanoscale with ion irradiation [8,9]. Even with these ongoing efforts at finding relevant applications there is still a lack of consensus about the nature of the metamagnetic transition in these films. To answer these questions there are currently parallel drives to understand the basic physics of this phenomena which employ methods such as two dimensional [10,11] and three dimensional [9,12] confinement, and probing techniques such as neutron scattering [4,13–16] and synchotron x-ray techniques [17,18].

Dozens of calculations of the electronic structure of FeRh in both phases have been published, starting with the first paper of Koenig [19], and including, but not limited to, later calculations [20–23]; all these calculations agree well among themselves. They show that the basic characteristics of the electronic structure, such as the density of states (DOS), $N(E)$, plasma frequency, ω_p, and the Fermi surface depend dramatically on the magnetic order. However, direct experimental verification is missing.

Optical properties of FeRh have also been studied by ellipsometery [24,25] and Fresnel reflectance measurements [26]. The ellipsometry techniques did not reveal a significant variation in the optical properties through the AF-F transition, since their focus is mainly on the visible region (1-3 eV). Indeed, first principles calculations [27] do not predict significant changes in the

#363802 https://doi.org/10.1364/OME.9.002870

Received 29 Mar 2019; revised 17 May 2019; accepted 22 May 2019; published 12 Jun 2019

Optical Materials EXPRESS

optical properties in this region. However, the same calculations demonstrated more significant changes in the near infrared region, which was subsequently confirmed by small changes (~1%) in reflectance and transmittance [26] in the near infrared (1.77 and 1.38 eV). Other than a few experiments like these, not much attention has been paid to possible optical signatures of magnetic ordering (apart from magneto-optical effects).

In this study, we report first principle calculations of the optical reflectivity, show that it is characteristically different in the two phases, and trace down these effects as being directly attributed to differences in the electronic structure. We also report experimental reflectance measurements covering a broad spectral range (0.5-3 eV) that demonstrate the theoretically predicted signature, a change of sign of the difference in reflectivity between the AF and FM phases near 0.8 eV.

2. Theory

All calculations were performed using the Linear Augmented Plane Wave method as implemented in WIEN2k package [28], and Perdew-Burke-Ernzerhof exchange-correlation functional [29]. We found the default WIEN2k setup (RMT = 2.43 aB in all cases, RKmax = 7, RGmax = 12, with one local p-orbital to relax the linearization errors) to be sufficiently accurate. For optical calculations, we have used a well-converged k-point mesh of $36 \times 36 \times 36$ points in the Brillouin zone. In Figs. 1(a) and 1(b) we show the calculated DOS:

We see that in the FM phase the spin-majority d-states of both Fe and Rh are essentially full, with only low-DOS sp-electrons left at the Fermi level, while both Fe and Rh states in the spin-minority channel are split by the cubic crystal field into a t_{2g} manifold, holding three electrons per ion, and an e_g manifold, holding two. The two are separated by a pseudogap, and the e_g state are already partially filled (by about 0.2 electrons per formula). Thus, overall DOS in the FM state is low in one spin (less than 10% of the total DOS), but sizeable in the other spin channel. The same is not true for the Drude plasma frequency, which is nothing but (to a constant factor) the DOS times the average squared Fermi velocity. Since the spin-majority (and only spin-majority) band is formed by light and fast sp-electrons, with the Fermi velocity much exceeding that of the d-electrons, the plasma frequency in this channel is actually *larger* than in the spin-minority one, by about 40%.

On the other hand, the Fermi level in the AF phase falls right in the crystal field pseudogap for either spin, as a result, the DOS is small *and* the plasma frequency is small. The calculated values are, respectively, ω_p=5.75 eV and 2.1 eV. Note that the static conductivity is proportional to ${\omega_p}^2/\gamma$, where γ is the Drude relaxation rate. Experimentally, the resistivity in the FM phase (90 μΩ.cm [3]) is smaller than in the AF one (150 μΩ.cm [3]), but not nearly by as much as their ratio of plasma frequencies squares (0.135) suggests. This was attributed to different scattering rate off spin fluctuations [30]. In the following, we assumed the Drude relaxation rates at room temperature to be 0.2 (1.1) eV for the FM (AF) phases so as to match the experimentally reported resistivities, using the calculated plasma frequencies.

Looking now at the interband transitions, we observe that there is dramatic difference there as well. The pseudogap in the AF phase is about 0.5 eV and the DOS is high on both sides (the states below and above are t_{2g} and e_g d-bands, respectively), so there is a rise in the interband absorption, starting at about 0.5 eV and reaching a strong maximum at 1.5 eV (see Fig. 1). On the other hand, as discussed above, the interband absorption in the FM phase comes mostly from the spin-minority bands, and the pseudogap is larger, so the corresponding maximum is weaker and displaced toward 2.5 eV. Via the Kramers-Kronig relations, both the difference in the Drude part and in the interband part affect the behavior of the reflectivity in the range of interest.

Indeed, it is well known that the Drude reflectivity at small energies $\hbar\omega << \gamma$ is given by the Hagen-Rubens formula Eq. (1),

$$R \approx 1 - 2\sqrt{2\omega/\sigma} \tag{1}$$

Optical Materials EXPRESS

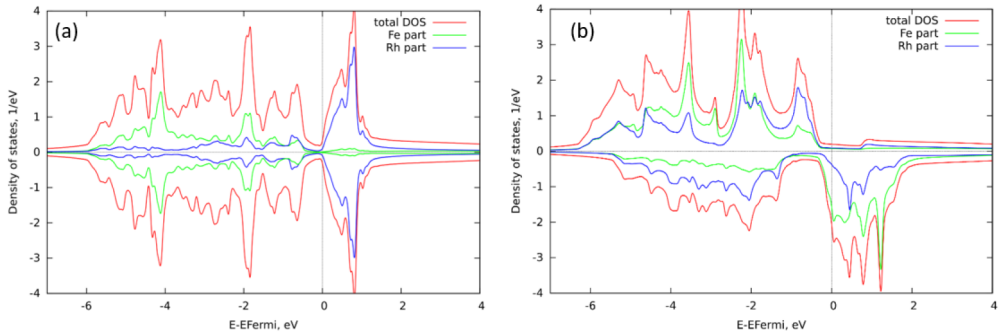

Fig. 1. Calculated density of states (DOS) for (a) the antiferromagnetic phase and (b) the ferromagnetic phase of FeRh. One can see in the AF plot a pseudogap between ~-0.45 and -0.08 eV, the states below being of the t2 g, and above of the eg character. In the FM plot, t2 g and eg states are not well separated in the majority channel; the eg states start roughly above -0.4 eV and extend to ~2 eV, while the t2 g ones span an interval between ~-5.5 and -1 eV.

while in the range $\gamma << \hbar\omega << \hbar\omega_p$ it is roughly a constant (Eq. (2),

$$R \approx 1 - \frac{2\gamma}{\omega_p} = 1 - 2\omega_p/\sigma \tag{2}$$

Given that $\sigma_{FM} > \sigma_{AF}$, but $(\omega_p/\sigma)_{FM} > (\omega_p/\sigma)_{AF}$, it is obvious that the two Drude reflectivities must cross. However, this crossing occurs at a very small frequency, smaller than 0.1 eV. The key to the observed crossover behavior lies in the different interband absorption: as Figs. 2(a) and 2(b) illustrate, the interband absorption in both cases, naturally, suppresses reflectivity. In the AF state it happens at lower frequencies, but the overall effect is stronger in the FM phase. This ensures that the two curve necessarily intersect at a frequency somewhat higher than the onset of the interband absorption in the AF phase; how much higher depends on the interband parts, in particularly the difference in the transport relaxation rates. However, as one can see in Fig. 2(a) , even dramatic variation between the $\gamma_{FM}=\gamma_{AF}$ limit and the $\gamma_{FM}>>\gamma_{AF}$ (as suggested by DC resistivity) only shifts the crossing point from ~0.8 to ~0.6 eV.

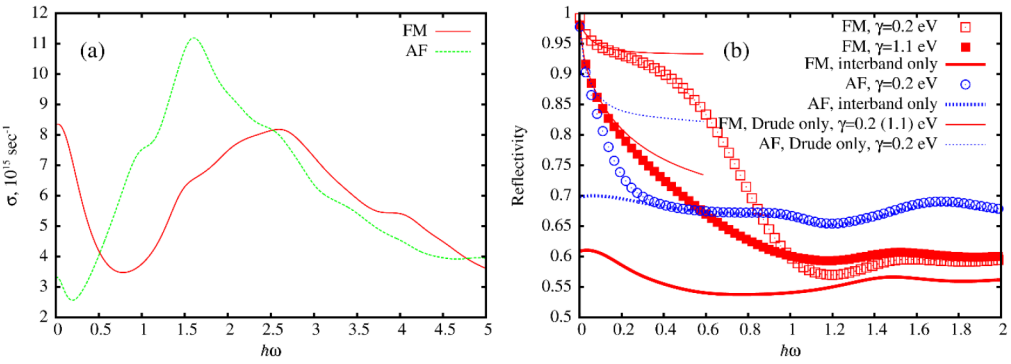

Fig. 2. (a) Calculated optical conductivity assuming the relaxation rate $1/\gamma$ is 0.2 eV for both cases. (b) Corresponding reflectivity, with the parameters as listed in the legend.

Optical Materials EXPRESS

3. Experiment

In order to verify the above theory and the main practical prediction, we measured the reflectance on FeRh films, grown by magnetron sputtering from a single $Fe_{50}Rh_{50}$ composition target. Samples were grown on single crystal MgO 001 oriented epi-ready substrates at 630C in an Ar atmosphere. The samples were then annealed under high vacuum at 730C for 1hr. Additional details on sample preparation can be found in previous work [15]. To characterize the sample quality the metamamagnetic transition was probed by magneto-optic Kerr effect (MOKE) (Figs. 3(a) and 3(b)). These measurements show a good quality antiferromagnetic (AF) to ferromagnetic (FM) transition occurring at T_c = ~385 K with a temperature hysteresis of ~20 K.

To investigate the optical properties of the transition two optical reflectance measurements were performed as the temperature was varied from 20 to 160 °C. In the first experiments, the incident reflectance of narrowband optical sources (in the visible through infrared: 0.62, 0.8, and 1.96 eV,) were individually measured as the temperature was varied through the AF-FM transition, as shown in Figs. 4(a), 4(b) and 4(c). The data at each wavelength show a transition near 120 °C and a hysteresis width of ~10-20 °C, corroborating the results shown by MOKE. The most interesting feature is the wavelength dependence of the reflectance. In the infrared (0.62 eV), the data show an increased reflectance during the transition from AF-FM phase, and on the other hand a decreased reflectance in the near infrared and visible (0.8 and 1.96 eV). These relative increases and decreases in the reflectance align very well with the first principle calculations shown in Fig. 2(b) by open markers and reproduced in a wider energy range in Fig. 2(a).

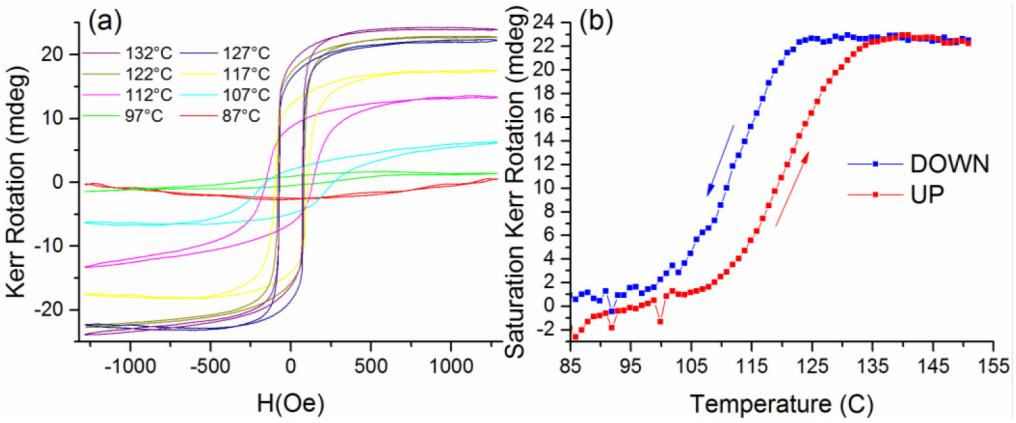

Fig. 3. Magneto-Optic Kerr Effect (MOKE) measurements of an FeRh film (a) Kerr rotation as a function of applied magnetic field H at temperatures from below the transition (87°C)) heating to above the transition (127°C)) The data at 87°C is the raw data without background subtraction (b) Saturation Kerr rotation (taken at H = 1250 Oe) as a function of temperature heating and cooling through the transition to display the temperature hysteresis.

To further examine the wavelength dependence of this effect, a second set of optical reflectance experiments addressed the spectral reflectance (from 0.5 to 3 eV) at normal incidence to the FeRh sample at discrete temperatures from 20 °C to 150 °C. These measurements were carried out with an Oxford MicrostatN fit with a quartz window into a Perkin Elmer Lambda 1050 spectrophotometer. The results show a significant change in optical reflectance as a function of wavelength as the sample is cooled (Fig. 5(c)) and heated (Fig. 5(d)) through its transition temperature. The large ΔR/R of the transition is also shown in Fig. 5(e) which plots the change in reflectance $\Delta R/R=(R_T-R_{20°C})/R_{20°C}$ as a function of temperature at selected wavelengths from the visible through infrared from the curves shown in Figs. 5(c) and 5(d). The plots show once again that the change in reflectance from the AF-FM state is positive for the infrared range, but

Optical Materials EXPRESS

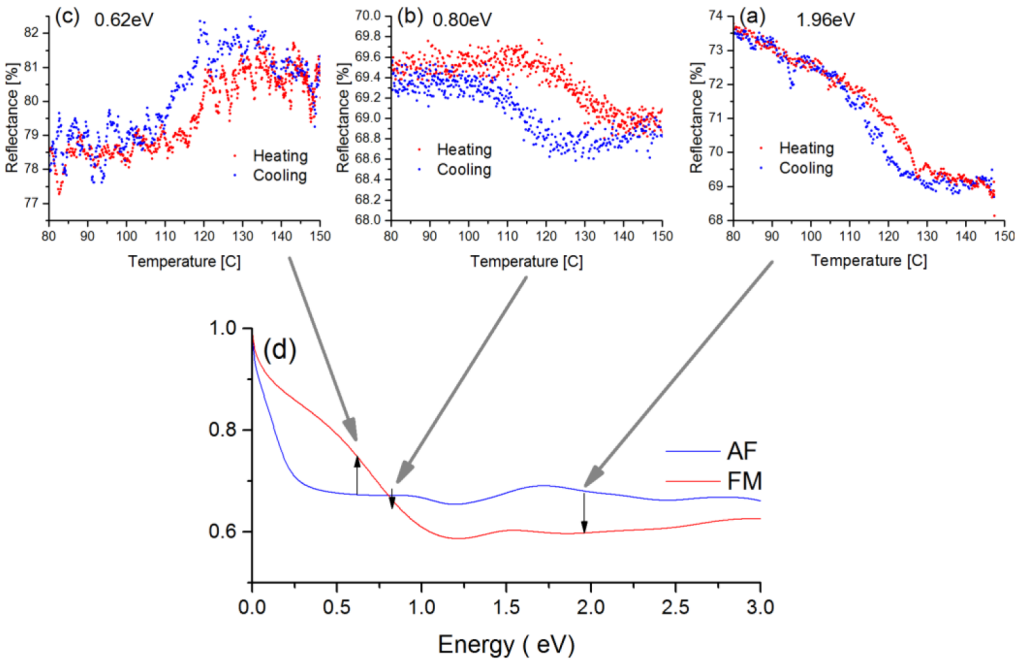

Fig. 4. Experimentally obtained CW laser reflectivity measurements of the metamagnetic transition measured at three different laser energies (a) 0.62 eV, (b) 0.80 eV and (c) 1.96eV

decreases with increasing photon energy until the change in reflectance is negative in the visible region. This characteristic crossover occurs at ~0.79 eV, which agrees surprising well with our modeled behavior of the AF-FM transition which is directly compared in Figs. 5(a) and 5(b).

When FeRh undergoes its metamagnetic transition not only does the magnetic ordering change from AF-FM but there is also a magnetostructural effect of a 1% volume change [31–34]. In thin film form this volume change is accommodated by an elongation of the c-axis of the unit cell and little to no change in the a-axis due to substrate interface pinning [32,33,35]. From the electronic structure point of view, the variations associated with these volumetric changes are negligible compared to those triggered by the changing magnetic order. Also correlated with the transition is a change in resistivity [3]. The latter, as discussed above, is important for understanding the optical properties and can be traced down to different magnon scattering in the two phases.

There has been a lot of interest in studying the metamagnetic transition with pump-probe optical techniques (i.e. pump-probe MOKE) [7,36–38], which can interrogate the transition on ultra-short timescales. Using the crossover in reflectivity shown here, these methods, if applied at different wavelengths, can point exactly where the AF-FM transition is occurring independent of the onset of thermally induced paramagnetic disorder (a pump induced Curie transition). Additionally, a crossover like this, occurring in an easily accessible wavelength region as shown here, provides additional input for verification theoretical calculations of key parameters of the electronic structure, such as the plasma frequencies.

To summarize, we have revealed, both theoretically and experimentally, that the dramatic difference in electronic structure between the antiferromagnetic and ferromagnetic phases of FeRh, leads to a characteristic crossover in the energy dependence whereby the reflectivity difference between the two phases completely changes sign at E=~0.79 eV (1400 nm), with a very close agreement between first principles calculations and optical spectra measured on FeRh films grown on MgO single crystal substrates. These measurements not only confirm the

Optical Materials EXPRESS

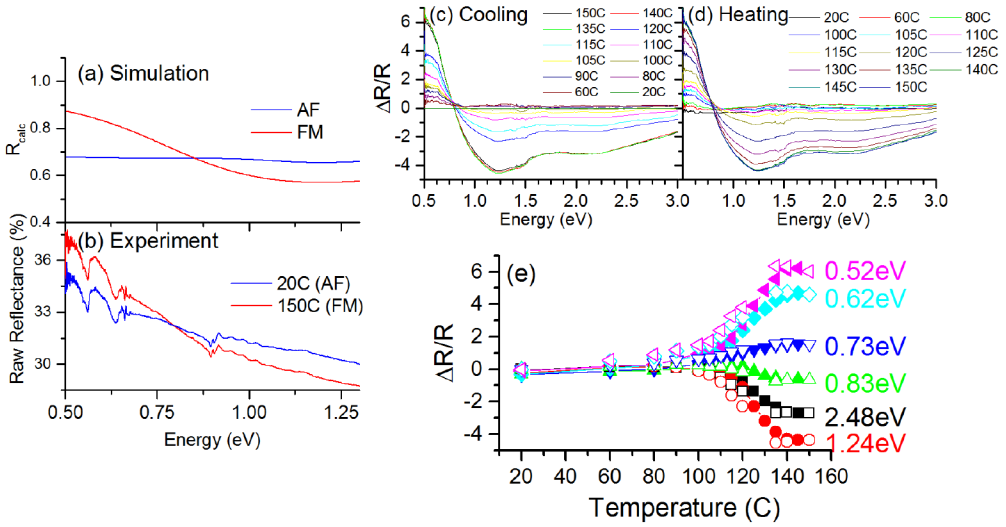

Fig. 5. Spectral reflectance measurements taken as a function of temperature across the metamagnetic transition with zero applied H-field. (a)&(b) Comparison between theoretically simulated (also shown in Fig. 4(d)) and experimentally acquired spectral reflectance of both phases. (c) Experimentally acquired reflectance as a function of temperature starting at high temperature, 150°C, and cooling to low temperature, 20°C. (d) Experimentally acquired spectral reflectance as a function of temperature starting at low temperature, 20°C, and heating to high temperature, 150°C. The lack of a change in the spectrum until the temperature reaches 120°C for the cooling case in (c), as opposed to spectral changes starting as high as 135°C for the heating case in (d), clarify the expected thermal hysteresis of the metamagnetic transition shown by MOKE in Fig. 3. (e) Plot showing ΔR normalized to R taken at temperatures ranging from 20°C - 150°C for photon energies ranging from 0.52 eV – 1.24 eV delineated by colors, marker shapes and corresponding labels. Shaded markers are points taken on heating while open markers indicate points taken on cooling.

calculated electronic structure of FeRh, but also reveal an effect that can be used for a fast and easy direct detection of the transition by probing the crossover in energy space, without resorting to complicated magneto optical probes which only show a signature of the magnetism. This also may be used as a unique probe of the dynamics of carriers by temporal studies in different regions, (from energies near the relaxation frequency to those above the plasma frequency) [39,40].

Funding

U.S. Naval Research Laboratory (NRL); Office of Naval Research (ONR); U.S. Department of Defense (DOD).

References

1. R. O. Cherifi, V. Ivanovskaya, L. C. Phillips, A. Zobelli, I. C. Infante, E. Jacquet, V. Garcia, S. Fusil, P. R. Briddon, N. Guiblin, A. Mougin, A. A. Ünal, F. Kronast, S. Valencia, B. Dkhil, A. Barthélémy, and M. Bibes, "Electric-field control of magnetic order above room temperature," Nat. Mater. **13**(4), 345–351 (2014).
2. X. Marti, I. Fina, C. Frontera, J. Liu, P. Wadley, Q. He, R. J. Paull, J. D. Clarkson, J. Kudrnovský, I. Turek, J. Kuneš, D. Yi, J. Chu, C. T. Nelson, L. You, E. Arenholz, S. Salahuddin, J. Fontcuberta, T. Jungwirth, and R. Ramesh, "Room-temperature antiferromagnetic memory resistor," Nat. Mater. **13**(4), 367–374 (2014).
3. Y. Lee, Z. Q. Liu, J. T. Heron, J. D. Clarkson, J. Hong, C. Ko, M. D. Biegalski, U. Aschauer, S. L. Hsu, M. E. Nowakowski, J. Wu, H. M. Christen, S. Salahuddin, J. B. Bokor, N. A. Spaldin, D. G. Schlom, and R. Ramesh, "Large resistivity modulation in mixed-phase metallic systems," Nat. Commun. **6**(1), 5959 (2015).

Optical Materials EXPRESS

4. S. P. Bennett, A. T. Wong, A. Glavic, A. Herklotz, C. Urban, I. Valmianski, M. D. Biegalski, H. M. Christen, T. Z. Ward, and V. Lauter, "Giant Controllable Magnetization Changes Induced by Structural Phase Transitions in a Metamagnetic Artificial Multiferroic," Sci. Rep. **6**(1), 22708 (2016).
5. I. Suzuki, M. Itoh, and T. Taniyama, "Elastically controlled magnetic phase transition in Ga-FeRh/BaTiO3(001) heterostructure," Appl. Phys. Lett. **104**(2), 022401 (2014).
6. M. Sharma, H. M. Aarbogh, J. U. Thiele, S. Maat, E. E. Fullerton, and C. Leighton, "Magnetotransport properties of epitaxial MgO(001)/FeRh films across the antiferromagnet to ferromagnet transition," J. Appl. Phys. **109**(8), 083913 (2011).
7. F. Pressacco, V. Uhlíř, M. Gatti, A. Nicolaou, A. Bendounan, J. A. Arregi, S. K. K. Patel, E. E. Fullerton, D. Krizmancic, and F. Sirotti, "Laser induced phase transition in epitaxial FeRh layers studied by pump-probe valence band photoemission," Struct. Dyn. **5**(3), 034501 (2018).
8. S. P. Bennett, A. Herklotz, C. D. Cress, A. Ievlev, C. M. Rouleau, I. I. Mazin, and V. Lauter, "Magnetic order multilayering in FeRh thin films by He-Ion irradiation," Mater. Res. Lett. **6**(1), 106–112 (2018).
9. R. C. Temple, T. P. Almeida, J. R. Massey, K. Fallon, R. Lamb, S. A. Morley, F. Maccherozzi, S. S. Dhesi, D. McGrouther, S. McVitie, T. A. Moore, and C. H. Marrows, "Antiferromagnetic-ferromagnetic phase domain development in nanopatterned FeRh islands," Phys. Rev. Mater. **2**(10), 104406 (2018).
10. T. A. Ostler, C. Barton, T. Thomson, and G. Hrkac, "Modeling the thickness dependence of the magnetic phase transition temperature in thin FeRh films," Phys. Rev. B **95**(6), 064415 (2017).
11. M. Loving, F. Jimenez-Villacorta, B. Kaeswurm, D. A. Arena, C. H. Marrows, and L. H. Lewis, "Structural evidence for stabilized ferromagnetism in epitaxial FeRh nanoislands," J. Phys. D: Appl. Phys. **46**(16), 162002 (2013).
12. V. Uhlíř, J. A. Arregi, and E. E. Fullerton, "Colossal magnetic phase transition asymmetry in mesoscale FeRh stripes," Nat. Commun. **7**(1), 13113 (2016).
13. R. Fan, C. J. Kinane, T. R. Charlton, R. Dorner, M. Ali, M. A. De Vries, R. M. D. Brydson, C. H. Marrows, B. J. Hickey, D. A. Arena, B. K. Tanner, G. Nisbet, and S. Langridge, "Ferromagnetism at the interfaces of antiferromagnetic FeRh epilayers," Phys. Rev. B: Condens. Matter Mater. Phys. **82**(18), 184418 (2010).
14. C. W. Barton, T. A. Ostler, D. Huskisson, C. J. Kinane, S. J. Haigh, G. Hrkac, and T. Thomson, "Substrate Induced Strain Field in FeRh Epilayers Grown on Single Crystal MgO (001) Substrates," Sci. Rep. **7**(1), 44397 (2017).
15. S. P. Bennett, A. Herklotz, C. D. Cress, A. Ievlev, C. M. Rouleau, I. I. Mazin, and V. Lauter, "Magnetic order multilayering in FeRh thin films by the He-ion irradiation," Mater. Res. Lett. **6**(1), 106–112 (2018).
16. S. P. Bennett, H. Ambaye, H. Lee, P. LeClair, G. J. Mankey, and V. Lauter, "Direct Evidence of Anomalous Interfacial Magnetization in Metamagnetic Pd doped FeRh Thin Films," Sci. Rep. **5**(1), 9142 (2015).
17. T. P. Almeida, R. Temple, J. Massey, K. Fallon, G. Paterson, T. Moore, D. McGrouther, C. H. Marrows, and S. McVitie, "Quantitative Differential Phase Contrast Imaging of the Magnetostructural Transition and Current-driven Motion of Domain Walls in FeRh Thin Films," Microsc. Microanal. **24**(S1), 936–937 (2018).
18. S. O. Mariager, L. Le Guyader, M. Buzzi, G. Ingold, and C. Quitmann, "Imaging the antiferromagnetic to ferromagnetic first order phase transition of FeRh," (2013).
19. C. Koenig, "Self-consistent band structure of paramagnetic, ferromagnetic and antiferromagnetic ordered FeRh," J. Phys. F: Met. Phys. **12**(6), 1123–1137 (1982).
20. L. M. Sandratskii and P. Mavropoulos, "Magnetic excitations and femtomagnetism of FeRh: A first-principles study," Phys. Rev. B: Condens. Matter Mater. Phys. **83**(17), 174408 (2011).
21. J. B. Staunton, R. Banerjee, M. dos, S. Dias, A. Deak, and L. Szunyogh, "Fluctuating local moments, itinerant electrons, and the magnetocaloric effect: Compositional hypersensitivity of FeRh," Phys. Rev. B **89**(5), 054427 (2014).
22. J. Kudrnovský, V. Drchal, and I. Turek, "Physical properties of FeRh alloys: The antiferromagnetic to ferromagnetic transition," Phys. Rev. B **91**(1), 014435 (2015).
23. R. Y. Gu and V. P. Antropov, "Dominance of the spin-wave contribution to the magnetic phase transition in FeRh," Phys. Rev. B **72**(1), 012403 (2005).
24. J. Y. Rhee and D. W. Lynch, "Optical properties of Fe-Rh alloys," Phys. Rev. B **51**(3), 1926–1927 (1995).
25. L.-Y. Chen and D. W. Lynch, "Ellipsometric studies of magnetic phase transitions of Fe-Rh alloys," Phys. Rev. B **37**(18), 10503–10509 (1988).
26. V. Saidl, M. Brajer, L. Horák, H. Reichlová, K. Výborný, M. Veis, T. Janda, F. Trojánek, M. Maryško, I. Fina, X. Marti, T. Jungwirth, and P. Němec, "Investigation of magneto-structural phase transition in FeRh by reflectivity and transmittance measurements in visible and near-infrared spectral region," New J. Phys. **18**(8), 083017 (2016).
27. M. A. Khan, C. Koenig, and R. Riedinger, "Interband dielectric constants in antiferromagnetic, ferromagnetic and paramagnetic phases of FeRh," J. Phys. F: Met. Phys. **13**(8), L159–L164 (1983).
28. P. Blaha, K. Schwarz, and G. K. H. Madsen, "WIEN2K, An Augmented Plane Wave+ Local Orbitals Program for Calculating Crystal Properties (TU Wien, Austria, 2001)," Isbn 3-9501031-1-2 2, 254 (2001).
29. J. P. Perdew, K. Burke, and M. Ernzerhof, "Generalized Gradient Approximation Made Simple," Phys. Rev. Lett. **77**(18), 3865–3868 (1996).
30. S. Mankovsky, S. Polesya, K. Chadova, H. Ebert, J. B. Staunton, T. Gruenbaum, M. A. W. Schoen, C. H. Back, X. Z. Chen, and C. Song, "Temperature-dependent transport properties of FeRh," Phys. Rev. B **95**(15), 155139 (2017).
31. H. Miyajima, S. Yuasa, and Y. Otani, "First-Order Magnetic Phase Transitions Observed in bct FeRh–Pt, Pd Systems," Jpn. J. Appl. Phys. **32**(S3), 232 (1993).

Optical Materials EXPRESS

32. J. M. Lommel, "Magnetic and electrical properties of FeRh thin films," J. Appl. Phys. **37**(3), 1483–1484 (1966).
33. J. S. Kouvel and C. C. Hartelius, "Anomalous magnetic moments and transformations in the ordered alloy FeRh," J. Appl. Phys. **33**(3), 1343–1344 (1962).
34. L. H. Lewis, R. Barua, and B. Lejeune, "Developing magnetofunctionality: Coupled structural and magnetic phase transition in $AlFe_2B_2$," J. Alloys Compd. **650**, 482–488 (2015).
35. J. M. Lommel and J. S. Kouvel, "Effects of mechanical and thermal treatment on the structure and magnetic transitions in FeRh," J. Appl. Phys. **38**(3), 1263–1264 (1967).
36. S. O. Mariager, F. Pressacco, G. Ingold, A. Caviezel, E. Möhr-Vorobeva, P. Beaud, S. L. Johnson, C. J. Milne, E. Mancini, S. Moyerman, E. E. Fullerton, R. Feidenhans'l, C. H. Back, and C. Quitmann, "Structural and Magnetic Dynamics of a Laser Induced Phase Transition in FeRh," Phys. Rev. Lett. **108**(8), 087201 (2012).
37. L. M. Sandratskii and P. Mavropoulos, "Magnetic excitations and femtomagnetism of FeRh: A first-principles study," Phys. Rev. B **83**(17), 174408 (2011).
38. G. Ju, J. Hohlfeld, B. Bergman, R. J. M. van de Veerdonk, O. N. Mryasov, J.-Y. Kim, X. Wu, D. Weller, and B. Koopmans, "Ultrafast Generation of Ferromagnetic Order via a Laser-Induced Phase Transformation in FeRh Thin Films," Phys. Rev. Lett. **93**(19), 197403 (2004).
39. I. Radu, C. Stamm, N. Pontius, T. Kachel, P. Ramm, J.-U. Thiele, H. A. Dürr, and C. H. Back, "Laser-induced generation and quenching of magnetization on FeRh studied with time-resolved x-ray magnetic circular dichroism," Phys. Rev. B **81**(10), 104415 (2010).
40. A. A. Ünal, A. Parabas, A. Arora, J. Ehrler, C. Barton, S. Valencia, R. Bali, T. Thomson, F. Yildiz, and F. Kronast, "Laser-driven formation of transient local ferromagnetism in FeRh thin films," Ultramicroscopy **183**, 104–108 (2017).